Astrophys Space Sci (2009) 322: 49–55
DOI 10.1007/s10509-008-9967-4

ORIGINAL ARTICLE

Image processing of radiographs in 3D Rayleigh-Taylor decelerating interface experiments

C.C. Kuranz · R.P. Drake · M.J. Grosskopf · H.F. Robey · B.A. Remington · J.F. Hansen · B.E. Blue · J. Knauer

Received: 20 June 2008 / Accepted: 8 December 2008 / Published online: 5 February 2009

Abstract This paper discusses high-energy-density laboratory astrophysics experiments exploring the Rayleigh-Taylor instability under conditions similar to the blast wave driven, outermost layer in a core-collapse supernova. The planar blast wave is created in an experimental target using the Omega laser. The blast wave crosses an unstable interface with a seed perturbation machined onto it. The perturbation consists of a 3D "egg crate" pattern and, in some cases, an additional longer wavelength mode is added to this 3D, single-mode pattern. The main diagnostic of this experiment is x-ray radiography. This paper explores an image processing technique to improve the identification and characterization of structure in the radiographic data.

Keywords Supernovae · Hydrodynamic instabilities · Laboratory astrophysics

1 Introduction

The experiments described in this paper are motivated by the mixing that occurs in a core-collapse supernova (SN). Of specific interest, is the core-collapse supernova SN1987A because there was a difference between the light curve data from the SN and the models at the time (Muller et al. 1991). Data collected from this SN showed higher velocities and earlier than expected x-ray emission of dense elements originating from the center of the star. This occurrence led to interest in further understanding the mixing between different elements and layers of the star.

Prior to the core-collapse and explosion, this type of supernova has a layered density structure with a dense iron core surrounded by layers of decreasing density with increasing radius (Arnett 1996). This results in a density gradient in the inward direction. Once the star explodes, a shock wave moves outward through the layers of decreasing density. The pressure is greatest just behind the shock front, which creates a pressure gradient in the radially outward direction. The opposition of the density and pressure gradients initiates the Rayleigh-Taylor (RT) instability (Rayleigh 1900; Taylor 1950). This instability grows following the initial, Richtmyer-Meshkov (Meshkov et al. 1997; Richtmyer 1960) response of the interface to the shock passage. At the times that this experiment is observed, it is dominated by the RT instability (Robey et al. 2003).

These experiments are designed to study the RT instability induced at the interface between the helium and hydrogen layers, the outermost layers of the star. Conditions similar to the SN are created using the Omega Laser (Boehly et al. 1995). The experiment is scaled so that it will have similar hydrodynamic evolution to that of the SN (Remington et al. 2006; Ryutov et al. 1999). These experiments build on past work and the fundamental dynamics and the specifics of the experimental scaling have been previously discussed (Drake et al. 2004; Kane et al. 1997; Kuranz et al. 2005, 2007; Robey et al. 2001). The primary diagnostic data produced in the experiments is radiographic images, from

C.C. Kuranz (✉) · R.P. Drake · M.J. Grosskopf
University of Michigan, Ann Arbor, MI, USA
e-mail: ckuranz@umich.edu

H.F. Robey · B.A. Remington · J.F. Hansen
Lawrence Livermore National Laboratory, Livermore, CA, USA

B.E. Blue
General Atomics, San Diego, CA, USA

J. Knauer
University of Rochester, Rochester, NY, USA

which one desires to extract quantitative measures of instability development, such as the location of the RT bubble tips and spike tips as well as to calculate the mass of features produced by the RT instability. The present paper is concerned with the analysis of data from a recent sequence of experiments, in which an improved diagnostic technique enabled us to obtain better diagnostic resolution, but introduced a challenging background feature into the experimental images. This background feature increases the difficultly in accurately locating and characterizing the features related to the RT instability. We describe and demonstrate here a method to remove enough of this background feature that improved analysis of the images is possible. We also illustrate a change in experimental technique that eliminates the background feature for future experiments, however, there is still a large amount of data that requires the image analysis technique described in this paper.

2 Experiment and experimental setup

The experimental target has two key components, high-density plastic layer and low-density foam. This establishes a density drop where the RT instability develops. The plastic layer is 150 μm thick and is composed mostly of polyimide ($C_{22}H_{10}O_5N_2$). It is followed by a few mm of carbonized resorcinol formaldehyde (CRF) foam. These main components of the target are shown in an exploded view in Fig. 1a. The densities of the materials are 1.41 g/cc and 50 mg/cc, respectively. On the rear surface of the polyimide a slot 75 μm deep, 230 μm wide and the length of the polyimide disk, 905 μm, is milled out of the piece. A strip of plastic that has been doped with bromine is glued into the slot. This strip is shown as the dark region of Fig. 1b. The density of the brominated plastic (CHBr) is 1.42 g/cc and the chemical composition is $C_{500}H_{457}Br_{43}$. Since the polyimide and CHBr have such similar densities the hydrodynamics of the experiment should not be affected substantially by the different materials. The purpose of doping the plastic with bromine is to provide contrast in the resulting side-on x-ray radiographs used to diagnose the experiment.

On the rear surface of the plastic piece, a 3D seed perturbation is machined. The basic pattern resembles an "egg crate" and is composed of two sine waves in orthogonal directions. The amplitude of the perturbation is 2.5 μm and the wavelength is 71 μm. In some experiments a multimode pattern is used to explore how the initial conditions affect the growth of the Rayliegh-Taylor instability. There are two multimode patterns that have a long wavelength sinusoid of either 212 μm or 424 μm in one direction. A mathematical model of one wavelength of the 2-mode perturbation with the additional long wavelength mode having a wavelength of 424 μm is shown in Fig. 1c.

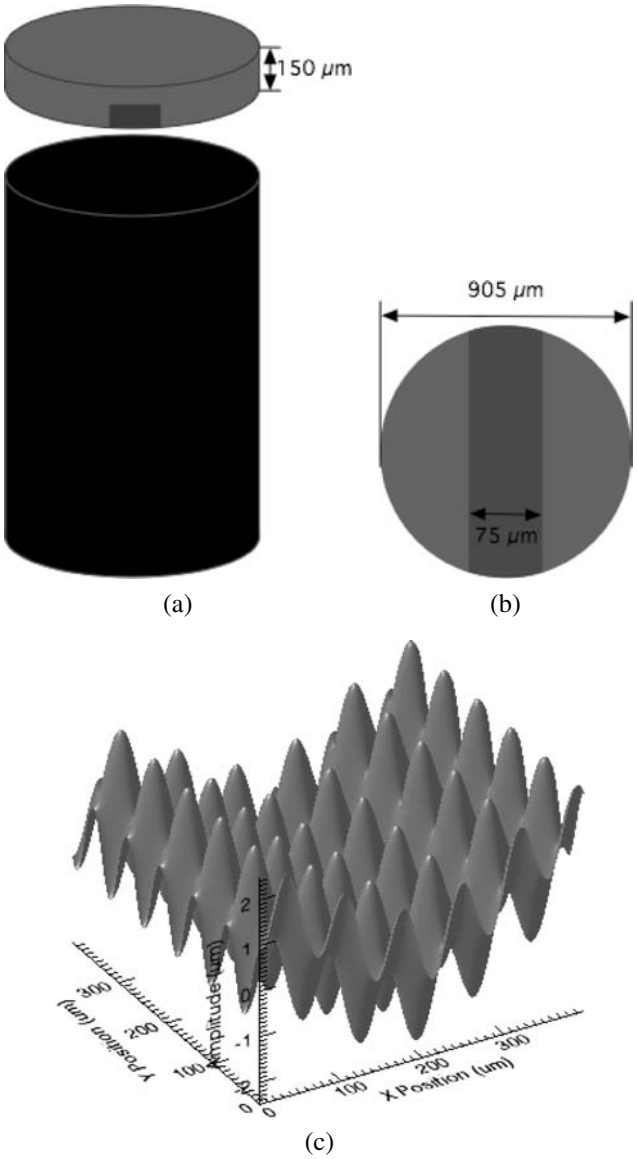

Fig. 1 (**a**) Exploded view of the key target components. The *gray* cylinder is the 150 μm thick, 905 μm diameter plastic piece and the black cylinder is the CRF foam that is 2–3 mm long. (**b**) The rear surface of the plastic piece where the *dark gray area* represents the CHBr. A slot 230 μm wide, 75 μm deep and the length of the component is milled out of the polyimide and the CHBr is glued into the slot. (**c**) This is an example of one of the perturbation types. This is a multimode pattern that has amplitude of 2.5 μm with orthogonal sine waves of 71 μm in wavelength and an additional mode of 424 μm in wavelength added in one direction. This image shows one full wavelength of the pattern that covers the entire disk

The plastic component, with the machined interface, and the foam are inserted into a polyimide tube with a nominal inner and outer diameter of 905 μm and 955 μm, respectively. The tube is attached to a conical, acrylic shield ∼21 mm at the opening and decreasing to ∼4 mm at the base. A gold wedge is attached to the shield on the side nearest the diagnostic. The purpose of the acrylic shield and gold

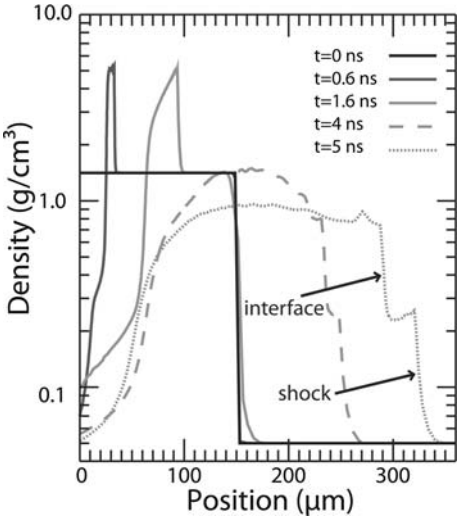

Fig. 2 A 1D Hyades plot of density vs. position for the experimental setup at several times. The laser irradiates the high-density material (plastic) and the interface of the low-density material (foam) is at 150 μm. This image shows the initial shock wave that is created by the ablation pressure from the laser and the blast wave that forms after the material begins to rarify. The blast wave crosses the interface at ∼2 ns and the evolution of the shock and interface is observed throughout the experiment

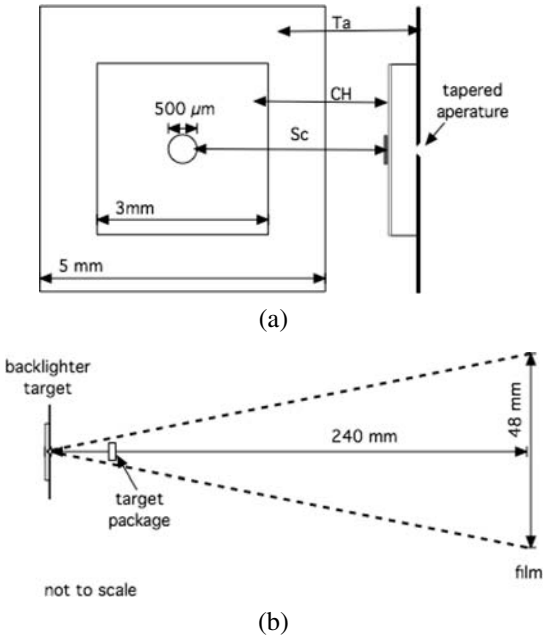

Fig. 3 (**a**) The backlighter target consists of a 500 μm, 12.5 μm thick Sc foil attached to a thin layer of plastic and mounted 500 μm from a 20 μm opening tapered to 10 μm in a piece of 5 mm × 5 mm Ta foil. (**b**) A schematic of the backlighter and diagnostic positions (not to scale) showing that, with the aperture specified above, there should be a uniform intensity from the x-rays over about ∼90% of the film

wedge are to prevent the ungated diagnostic used in the experiment from detecting emission from the hot plasma created when laser beams create the initial shock wave. There is also a gold washer at the base of the shield and underneath the edges of the plastic disk to prevent plasma from leaking out of the base of the shield. The gold washer has an outer diameter of 2.5 mm and an inner diameter of 1 mm, and it is covered with a thin layer of plastic and is not irradiated by the laser.

Ten Omega laser beams irradiate the plastic piece of the target with a 1 ns square pulse. The laser beams have an energy of ∼450 J/beam and pass through a distributed phase plate producing spot size of 820 μm FWHM. The beam is smooth overall with speckles on the 5-μm scale. The laser beams create an intensity of $\sim 10^{15}$ W/cm^2 and an ablation pressure of ∼50 Mbars or ∼50 million atmospheres. This ablation pressure creates a shock wave in the plastic layer. The propagation of this shock wave is shown at several times in Fig. 2. This plot shows density vs. position from a 1D Hyades (Larsen and Lane 1994) simulation.

The black line, which represents $t = 0$ ns, shows the initial condition of the target; 150 μm of dense material followed by the less dense foam (50 mg/cm^3). At 0.5 ns, the sharp increase in density at a position of 50 μm indicates that a shock wave has formed in the plastic layer. The laser pulse ends at 1.0 ns. By 1.5 ns, the shocked material has started to expand (decompress) which leads to a rarefaction wave moving to the right. This rarefaction quickly overtakes the shock turning the shock into a blast wave moving towards the interface between the plastic and foam. The blast wave crosses the density drop at the interface at ∼3 ns, which causes a forward shock to launch into the foam, seen clearly at 5 ns in the simulation. This experiment observes the evolution of the shock and interface.

The primary diagnostic is side-on, x-ray radiography. A second target, seen in Fig. 3a, is a point projection pinhole backlighter used to create 4.32 keV x-rays for the purpose of radiography. The target consists of a 50 μm, 5 mm square Ta foil with a pinhole aperture of 20 μm tapered to 10 μm. A 12.5 μm thick, 500 μm diameter disk of Sc is mounted on a 50 μm thick piece of CH. The CH mounted with Sc is positioned 500 μm from the Ta substrate. Three or 4 additional laser beams irradiate the Sc foil in a 1 ns pulse. The beams have an energy of ∼400 J/beam and a converging spot size of 1000 μm. The purpose of the large spot size is to overfill the Sc foil in order to tamp the metal plasma and prevent it from expanding laterally beyond the edge of the Ta foil (Kuranz et al. 2006). This backlighter target creates a directed flow of 4.32 keV x-rays to radiograph the target. The x-rays from the backlighter pass through the target and are recorded on x-ray film loaded in an ungated static pinhole camera array (SPCA).

The SPCA is loaded with a 12.5 μm thick piece of Ti to filter out high energy x-rays above the cold K-edge at 4.493 keV that may be created in the experiment. It is also loaded with a 500 μm piece of Be to filter out low energy

x-rays to reduce the amount of noise in our images. In these experiments the SPCA was loaded with Agfa D7 x-ray film. After the experiment the film is digitized with a resolution of 22 µm per pixel on the film. The film is 240 mm from the backlighter target as shown in Fig. 3b. From a geometric-optics perspective, this distance and the aperture of the pinhole should create a relatively flat intensity over an area of ∼18 cm^2 and area of the entire film is ∼20 cm^2. Thus, the intensity from the backlighter should be flat over roughly 90% of the film.

3 Results and discussion

Figure 4a shows a radiographic image taken at 21 ns after the laser beams irradiated the target. This particular target had a multimode seed perturbation with an additional wavelength of 424 µm in one direction. In this image the interface and shock are moving to the right. The long, dark fingers are spikes due to the Rayliegh-Taylor instability. Bubbles of foam are in between the spikes of brominated plastic. The gold grid, with a wire period of 63 µm, can be seen in the upper right hand corner. The dark portion of the image on the far right is the edge of the gold covered acrylic shield. The various thin, white streaks on the image are scratches on the film.

For this experimental series several targets are imaged at different times after the initial laser pulse. The resulting radiographs are similar to the one seen in Fig. 4a. It is important to fully characterize the features described above in each image. Some examples of characterization are finding the location of the tip of the spike and the tip of the bubble as well as finding the amount of mass in a spike, bubble or the entire interface region. This information can be taken from several radiographic images at several different times, which allows the study of the evolution of the RT instability.

Figure 4b is an image of the entire piece of film, which is about 50.8 mm in diameter. An interesting feature in this image is the large spot, outlined by a black circle, that is a little over 1 mm in diameter in the target plane and ∼20 mm on the film. This spot appears on all of our data images under similar conditions although its location, brightness and shape vary. Since the spot is circular it is thought that it is coming through the pinhole. The spot is apparently produced by very-high-energy photons or electrons, absorbed very weakly by the target, because it reduces the contrast of the observed structures in the image. The size of the pinhole and its position in relation to the experiment should provide a mostly flat illumination as discussed earlier in this paper and shown in Fig. 3b. One can look at the unshocked foam, where the intensity in the image should be relatively uniform to see that this is not the case in this image. A 1D

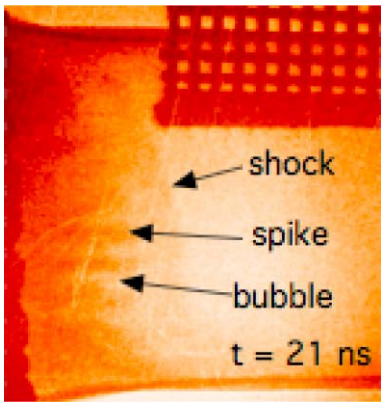

(a)

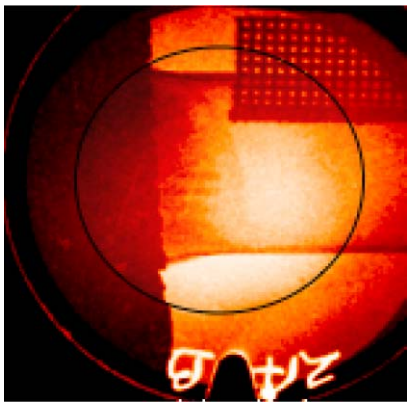

(b)

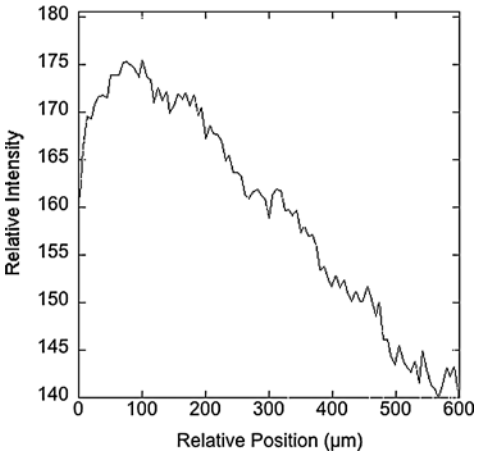

(c)

Fig. 4 (**a**) An x-ray radiograph of an experiment that had a multimode perturbation machined onto the interface of the target. This multimode pattern had an additional wavelength of 424 µm. The shock wave and interface are moving to the right in this image. (**b**) This is the entire piece of film from this experiment. Note the circular spot that is roughly in the center of the image. (**c**) This is a 1D profile through the unshocked foam region. This plot of relative intensity vs. relative position should be uniform, but there is a prominent drop off due to the bright, circular emission on the film

profile from the unshocked region in the foam is shown in Fig. 4c. This plot shows the relative pixel intensity vs. relative position in the unshocked foam. The fluctuations in the profile probably result from Poisson noise due to the limited number of x-ray photons. In similar, previous data we have shown this to be the primary source of noise (Kuranz et al. 2006).

This spot is of unknown origins and diminishes the contrast in the image. Eliminating the bright area from the image would greatly improve the image contrast and make the spike and bubble tips as well location of the shock front less obscured by the bright area on the radiographic image. Also, when calculating the mass of a spike, another way of analyzing this data, the background spot would lead to erroneous measures of mass. One possible way to remove much of the spot is to invert the image to k-space using a Fast Fourier transform (FFT), subtract the modes that are related to the spot in the image, and then invert the image back to optical density space. These operations were performed using the Interactive Data Language (IDL). When an FFT is taken of a 2D array in IDL there are 4 elements in the power spectrum that corresponds to each 2D mode in the image, the real and imaginary parts of k_x and k_y. To remove the spot, one must identify the modes that correspond to it and subtract them in Fourier space.

The image shown in Fig. 4a contains numerous modes of varying amplitudes. The spot is roughly 1 mm in diameter in the target plane or covers about half of the image. As an approximation, assume this relates to a single low-order mode with a wavelength the entire length of the image. The four elements for that mode are then set to zero in the array of the power spectrum. Then the power spectrum is inverted to optical density space and then image should be of better quality. The image with the long wavelength mode removed is shown in Fig. 5a and a magnified image of the film is seen in Fig. 5b. Even in this approximation the quality has improved from the initial image both in contrast and intensity uniformity. There is still a variation in the unshocked foam region, however, it is smaller and of less intensity than the original spot. This can be seen by the 1D profile taken from the image of Fig. 5b, shown in Fig. 5c. Similar to Fig. 4c, this plot is the relative pixel intensity vs. the relative position in unshocked foam. There also remains a variation outside of the shock tube, which can be seen in the image of the entire piece of film, Fig. 5a. The fact that the spot was not completely removed means that the spot is not entirely sinusoidal in nature. The majority of the spot can be modeled as a 2D sinusoid; however, when that is subtracted some smaller wavelength components of the spot still remain and can be seen on the image. Largely, the image with the long wavelength component of the bright feature removed is much improved.

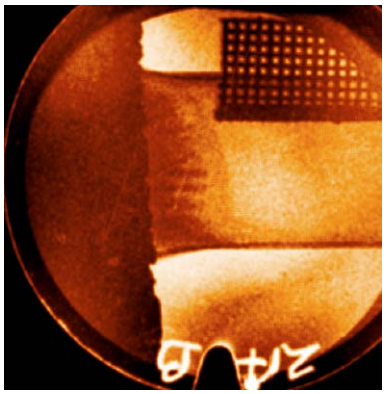

(a)

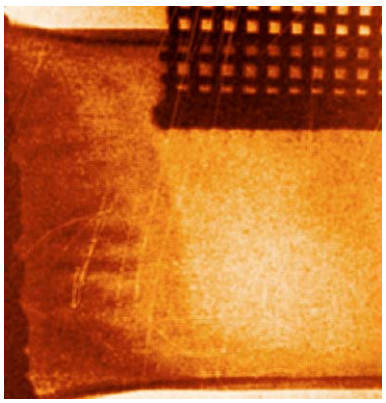

(b)

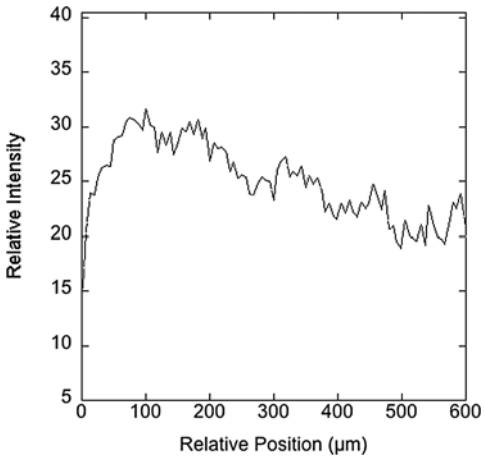

(c)

Fig. 5 (**a**) This is the x-ray radiograph shown in Fig. 4b with the bright spot mostly removed using the FFT. (**b**) This expanded image shows that the bright area is greatly diminished. (**c**) A 1D profile through the unshocked foam region shows a much flatter intensity that in Fig. 4c

Another way to remove the spot is to use the 1D profile in the unshocked foam from Fig. 4c in order to model the structure of the spot in the film. Then this modeled spot can be subtracted from the image. It is assumed that spot is circular and the 1D profile is essentially rotated 360° to create this model. The center of the spot is estimated by looking at the

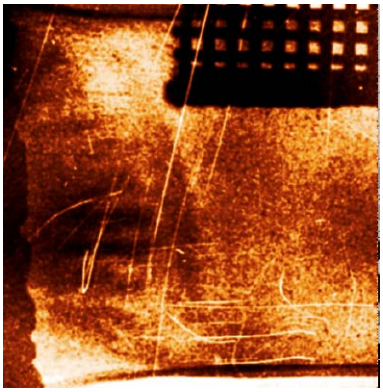

(a)

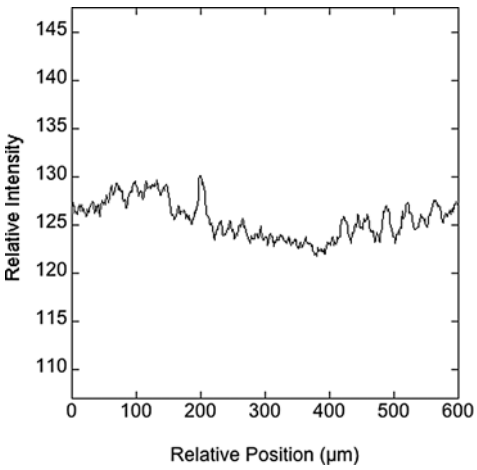

(b)

Fig. 6 (**a**) This is the x-ray radiograph similar to the one shown in Fig. 4a with the bright spot mostly removed using the spot modeling technique. (**b**) A 1D profile through the unshocked foam region shows a much flatter intensity that in Fig. 4c

brightest area on the radiographic image as well as measuring the overall size of the spot and taking the midpoints. If the center of the spot, which we are assuming to be the maximum intensity, lies outside of the unshocked foam region it is difficult to accurately model the spot. This is because there is variation in the shocked material due to the RT instability and one cannot ascertain how much of the pixel intensity is due to the background spot. However, this method captures the general size and variation in the background feature.

The result from subtracting the modeled spot from the radiographic image is shown in Fig. 6a. As with the FFT method, the important features in the radiograph, the spike and bubble tips as well as the shock front, are clearer than in original radiograph. Also, a 1D profile in the unshocked foam section from the resulting image is shown in Fig. 6b. Again, this is relatively flat compared to Fig. 4c.

It is important to compare the results of both methods as they can both be utilized for different purposes. Important features can be seen more clearly in Fig. 5b than in Fig. 6. For this image it would be best to use the FFT method to find the location of the spike tip, bubble tip and shock front. Also, when the center of the background spot is located far from the unshocked foam region the spot subtraction method would become less accurate, as discussed previously, and it would also be best to use the FFT method. However, the spot subtraction method proves to be more useful in certain cases. In observing the RT instability, it is of great interest to be able to study the flow of mass due to the instability. For instance, one can calculate the amount of mass in the spikes using method described by Hansen et al. (2007). The method described uses the pixel intensity as one parameter in calculating the mass from a radiographic image. If an image had the background feature shown in this paper the pixel intensity would not truly reflect the mass of the material of that pixel. In this case, modeling the spot and subtracting it from the image would yield more accurate pixel intensities and therefore masses. Since the method of "removing" the mode includes setting the value of that mode to zero this method changes the pixel intensity as can be seen by comparing the 1D profiles in Figs. 4b and 5b. Therefore, when calculating the amount of mass of a specific region in the image, the spot subtraction method is more precise.

As mentioned previously, the cause of this spot is unknown, although it plausibly may result from laser-plasma-interaction processes that can produce very energetic electrons. Accordingly, it was suggested that the spot would not appear if the beams irradiating the pinhole backlighter target came to the backlighter foil as a divergent beam, having passed through its focus, as opposed to a converging focus. (The diverging beam is more uniform than the converging one.) This hypothesis was tested on another experimental day using the same experimental setup except that the backlighter beams were diverging and the film was D8, another type of Agfa film, instead of D7. The resulting image shown in Fig. 7a does not show a bright spot. A 1D profile of the relative intensity vs. relative position in the unshocked foam is shown in Fig. 7b. The profile is flatter overall. The use of D8 film rather than D7 cannot explain the disappearance of the spot, since D8 is more sensitive than D7. If the spot existed it would only appear brighter on D8. That same experimental day D7 film was used and it did not show a bright spot either, however, the overall quality of the film was poor due to low signal from our backlighter.

4 Conclusions

Recent experiments, motivated by supernovae hydrodynamics, have observed growth due to the RT instability from 3D multimode initial conditions. The quality of the resulting radiographic images is variable. This is due to a bright spot

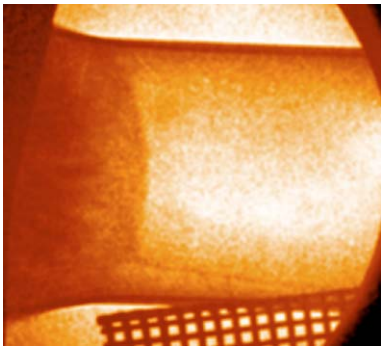

(a)

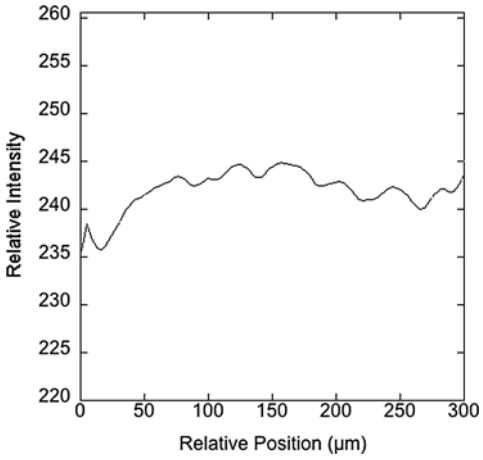

(b)

Fig. 7 (**a**) This x-ray radiograph was taken under conditions similar to the previous radiograph except that the beams that irradiated the backlighter target came to a diverging focus whereas in the previous image the backlighter beams came to a converging focus. (**b**) A 1D profile in the unshocked foam is more uniform than in Fig. 4c as is predicted by out backlighter geometry shown in Fig. 3

of unknown origin that appears on the film in some images, reducing the contrast of the data. However, the data can be made more suitable for quantitative analysis by taking the FFT of the image and removing the dominant modes that correspond to the global scale of the spot. An alternative method is to model the structure of the spot and subtract it from the image. Both of these methods improve quality of the radiographic image. Which method should be used depends on what type of further analysis will be implemented on the image pertaining to the RT instability. In limited tests, the spot has not appeared when the backlighter beams are diverging rather than converging. The data analysis approach discussed here will enable more accurate determination of the structure produced by the instabilities. The change in experimental technique should lead to improved data in future experiments.

Acknowledgements The authors would like to acknowledge Nick Lanier and Chuck Sorce for useful technical discussions. Also the authors would like to recognize the support of the Omega operations team and the Michigan target fabrication team and General Atomics component fabrication group for their work on the experimental targets. Financial support for this work included funding from the Stewardship Science Academic Alliances program through DOE Research Grant DE FG03-99DP00284, and through DE-FG03–00SF22021 and other grants and contracts.

References

Arnett, W.D.: Supernova and Nucleosynthesis. Princeton University Press, Princeton (1996)
Boehly, T.R., et al.: Rev. Sci. Instrum. **66**, 508 (1995)
Drake, R.P., et al.: Phys. Plasmas **11**, 2829 (2004)
Hansen, J.F., Robey, H.F., Klein, R.I., Miles, A.R.: Astrophys. J. **662**, 379 (2007)
Kane, J., et al.: Astrophys. J. **478**, L75 (1997)
Kuranz, C.C., et al.: Astrophys. Space Sci. **298**, 9 (2005)
Kuranz, C.C., et al.: Rev. Sci. Instrum. **77**, 10E327 1 (2006)
Kuranz, C.C., et al.: Astrophys. Space Sci. **307**, 115 (2007)
Larsen, J.T., Lane, S.M.: J. Quant. Spectrosc. Radiat. Transfer **51**, 179 (1994)
Meshkov, E., et al.: In: 6th International Workshop on the Physics of Compressible Turbulent Mixing, Marseille, France (1997)
Muller, E., Fryxell, B., Arnett, D.: Annu. Rev. Astron. Astrophys. **251**, 505 (1991)
Rayleigh, L.: Scientific Papers II. Cambridge University Press, Cambridge (1900)
Remington, B.A., Drake, R.P., Ryutov, D.D.: Rev. Mod. Phys. **78**, 755 (2006)
Richtmyer, D.H.: Commun. Pure Appl. Math. **13**, 297 (1960)
Robey, H.F., et al.: Phys. Plasmas **8**, 2446 (2001)
Robey, H.F., Zhou, Y., Buckingham, A.C., Keiter, P., Remington, B.A., Drake, R.P.: Phys. Plasmas **10**, 614 (2003)
Ryutov, D.D., Drake, R.P., Kane, J., Liang, E., Remington, B.A., Wood-Vasey, M.: Astrophys. J. **518**, 821 (1999)
Taylor, S.G.: Proc. R. Soc. A **201**, 192 (1950)